Graefe's Arch Clin Exp Ophthalmol
(2005) 243: 774–779

CLINICAL INVESTIGATION

DOI 10.1007/s00417-004-1118-1

Stefano Da Pozzo
Pierluigi Iacono
Roberta Marchesan
Anna Fantin
Giuseppe Ravalico

Scanning laser polarimetry with variable corneal compensation and detection of glaucomatous optic neuropathy

Received: 31 August 2004
Revised: 17 November 2004
Accepted: 10 December 2004
Published online: 9 March 2005

None of the authors have any financial or proprietary interest with products cited in the text

S. Da Pozzo (✉) · P. Iacono ·
R. Marchesan · A. Fantin · G. Ravalico
Eye Clinic, Ospedale Maggiore,
University of Trieste,
Piazza dell'Ospedale 1,
34129 Trieste, Italy
e-mail: stefano34127@lycos.it
Tel.: +39-40-772449
Fax: +39-40-772449

Abstract *Background:* The aim of this study was to evaluate the ability of scanning laser polarimetry (SLP) parameters provided by commercially available GDx with variable corneal compensator (VCC) to discriminate between healthy and glaucomatous eyes. *Methods:* Sixty-five healthy and 59 glaucomatous age-matched patients underwent a complete ophthalmological evaluation, an achromatic automated perimetry (AAP), and SLP with GDx-VCC. One randomly selected eye from each subject was considered. All glaucomatous eyes had reproducible visual field defects. Mean values (± SD) of all SLP-VCC parameters measured in the two groups were compared. Area under receiver operating characteristics (AUROC) curve and sensitivities at predetermined specificities of ≥80% and ≥95% for each single parameter were calculated. Moreover, the nerve fiber indicator (NFI) diagnostic accuracy was evaluated calculating positive, negative, and interval likelihood ratios (LRs) at different cutoff values. *Results:* All SLP parameters were significantly different between the two groups (p<0.001). The NFI showed the best AUROC curve (0.938, SE 0.02) whereas temporal, superior, nasal, inferior, temporal (TSNIT) average was second best (0.897, SE 0.03), and normalized superior area was third (0.879, SE 0.04). At fixed specificity ≥95%, sensitivities ranged from 22% to 79.7% whereas for values ≥80%, sensitivities were in the 44.1–89.8% range. At a cutoff NFI value of 30, positive LR was 17.6 (95% CI: 5.8–53.6) and negative LR was 0.19 (95% CI: 0.11–0.33). Interval LRs for NFI showed that values ≤20 or >40 were associated with large effects on posttest probability. *Conclusions:* SLP-VCC allows good discrimination between healthy and glaucomatous eyes. New software-provided parameters NFI, TSNIT average, and normalized superior and inferior areas appear to be reliable in the evaluation of glaucomatous disease. In particular, after evaluation on interval LRs, the NFI showed a high diagnostic accuracy for values ≤20 or >40.

Keywords Glaucoma · Scanning laser polarimetry · Corneal birefringence

Introduction

Glaucoma is a progressive optic neuropathy that selectively affects retinal ganglion cells (RGC). Histologic and longitudinal studies provide the evidence that structural damage precedes functional loss [11, 16, 17, 24]. In fact, an RGC loss of at least 40% may occur before any glaucoma-related change can be detected by standard automated perimetry [17]. Imaging technology allows clinicians to obtain in vivo quantitative and reliable measurements of peripapil-

lary retinal nerve fiber layer (RNFL) thickness by means of scanning laser polarimetry (SLP). Polarized laser light passing through tissues with physical properties of form birefringence undergoes a retardation that is linearly related to thickness in a primate model [27]. With respect to previous versions, the most recent instrument is coupled with variable corneal compensation (VCC) [32]. This innovation provides a customized compensation of anterior segment birefringence in which incomplete removal represented a potential source of spurious measurements on SLP with a fixed corneal compensator (FCC) [1, 7, 12, 29, 30]. Previous reports demonstrated how this fact limited the clinical significance of RNFL thickness measurements [2, 4, 8, 13, 28, 31]. Several studies have confirmed that SLP- have improved significantly both the structure–function relationship [18] and the ability to discriminate normal from glaucomatous eyes with respect to SLP-FCC [3, 5, 14, 15, 19–21, 25]. Moreover, SLP-VCC introduced new parameters such as nerve fiber indicator (NFI), ellipse (temporal, superior, nasal, inferior, temporal; TSNIT) average and standard deviation, normalized superior area (NSA) and normalized inferior area (NIA) in the attempt to provide more reliable indicators of the disease.

The aim of this study was to evaluate the diagnostic ability of SLP-VCC parameters to discriminate adequately healthy from glaucomatous eyes.

Methods

We selected patients among those referred to the Glaucoma Unit at Trieste University Eye Clinic between January and July 2004 for periodical scheduled visits.

Inclusion criteria were as follows:

- Peripapillary RNFL thickness evaluation by means of SLP-VCC
- Good quality polarimetric images (quality score ≥8 as automatically provided by device software)
- Good quality automated achromatic perimetry (AAP) performed at ±1 month from SLP (further details on AAP interpretation are presented later)
- Refractive error within the ±4 spherical diopter range, with less than ±2 cylinder diopter

Exclusion criteria were as follows:

- Best-corrected visual acuity (BCVA) <20/40
- Corneal or lens opacity significantly interfering with clinical, AAP, or SLP examination
- Significant peripapillary atrophy falling under ellipse measurement, tilted disc, uveitis, significant vitreous floaters, or diffuse or localized retinal or macular disease
- Inability to perform reliable AAP (fixation losses, false-positive or false-negative rates greater than 20%) or SLP (poor fixation, inattentive patients)

Each patient underwent a complete ophthalmological examination. A single eye from each enrolled subject was selected randomly for inclusion if both met the eligibility criteria. BCVA was assessed on a standard ETDRS chart. At slit lamp, the anterior segment was examined and gonioscopy and Goldmann applanation tonometry performed. The optic disc was studied by stereo biomicroscopy with the aid of a +90 D lens after pupil dilation. AAP was performed with the Humphrey Field Analyzer (Humphrey Systems, Dublin, CA, USA), 24-2 program, SITA standard strategy. Healthy subjects were recruited among staff members, friends or spouses of patients, or normal volunteers. They all had normal AAP [mean deviation (MD) and pattern standard deviation (PSD), values within 95% confidence limits; and glaucoma hemifield test (GHT), within normal limits] as well as intraocular pressure <21 mm Hg, healthy optic disc with intact neuroretinal rim, no history of ocular disease, and no family history of glaucoma.

Glaucomatous optic neuropathy was defined as cupping, rim notching, or diffuse thinning. On AAP, defects were classified as glaucomatous when either GHT was labeled as outside normal limits or a PSD probability of less than 5% was found. For the purpose of statistical analysis, MD and PSD were considered. All glaucomatous patients had at least two previous AAP and reproducible visual field defects.

SLP-VCC was performed with the commercially available device (GDx-VCC, software 5.3.4; Laser Diagnostic Technology, San Diego, CA, USA) using an eight-pixel-wide (approximately 0.4 mm in an emmetropic eye) circular calculation area with inner diameter of 54 pixels (approximately 2.5 mm in an emmetropic eye) centered on the optic disc. The first reading was obtained to measure and compensate anterior segment birefringence. The correct positioning of the macular circle was checked after its acquisition. Then, the second reading provided values of RNFL parameters under the calculation area. Before accepting any reading, the correct circle placement on the inner margin of the peripapillary scleral ring was checked on the reflectance image. On both readings, maximum effort was paid to obtain high-quality scans, and all eyes had to pass the four-scan quality checks performed by software (alignment, fixation, refraction, and illumination). The operator assisted patients in keeping their heads as vertical as possible during scanning sessions in order to avoid artifacts deriving from head tilt. The correct positioning of the ellipse on the inner margin of the peripapillary scleral ring was rechecked on all eyes by a trained technician (RM). The image to be analyzed was created from three images ob-

Table 1 Mean values (± SD) of age, mean deviation (MD), and pattern standard deviation (PSD) in normal and glaucomatous eyes.

	Normal (n=65)	Glaucoma (n=59)	P value*
Age (years) mean (± SD)	64.6±7.5	67.1±9.1	<0.09
Visual field MD (dB) mean (± SD)	−0.34±1.67	−7.66±6.19	<0.001
Visual field PSD mean (± SD)	1.51±0.65	7.46±4.18	<0.001

*t test

tained in each subject. Scans with evidence of atypical pattern on the thickness map were excluded from the study.

Parameters considered were ellipse average and standard deviation (TSNIT average and SD), superior and inferior average (SA, IA), NFI, superior and inferior ratio (SR, IR), superior/nasal ratio (S/N), maximum modulation (MM), superior and inferior maximum (SM, IM), ellipse modulation (EM), and normalized superior and inferior area (NSA, NIA). NFI is a software-generated parameter calculated using a support vector machine algorithm based on several RNFL measures that assigns a value from 0 to 100 to each examined eye. The higher the NFI, the greater the likelihood that the eye is glaucomatous. Mean values (± SD) of each parameter were compared at t test in order to check differences between healthy and glaucomatous eyes. Bonferroni correction was applied based on the number of comparison (14 comparisons: approximately α=0.0036). Symmetry was not considered since in previous studies its significance resulted to be minimal [8, 14, 15, 29]. For each parameter, receiver operating characteristic (ROC) curves were generated and sensitivities at fixed specificity (≥80% and ≥95%) calculated. ROC curves show the trade-off between sensitivity and 1-specificity. An area under the ROC curve (AUC) of 1 represents perfect discrimination whereas an AUC of 0.5 represents chance discrimination.

For NFI, positive and negative likelihood ratios (LRs) were also calculated using the manufacturer's suggested cutoff of 30 (that is supposed to separate "within normal limits" from "borderline" eyes) and other different, arbitrarily selected cutoffs. LR is the probability of a given test result in those with disease, divided by the probability of the same test result in those without the disease [6]. The classification of the effect of LRs of different magnitudes on the posttest probability of disease proposed by Jaeschke et al. [10] was used so that large effect on posttest probability was associated with LRs higher than 10 or lower than 0.1. Moreover, interval LRs were also calculated to weigh the effect of different NFI range values on posttest probability. In all cases, LR values were provided with

Table 2 Retinal nerve fiber layer measurements (mean ± SD) in healthy and glaucomatous eyes on scanning laser polarimetry and variable corneal compensator (SLP-VCC)

	Healthy eyes (n=65)	Glaucomatous eyes (n=59)	P value*
NFI	21.1±6.5	54.0±23.1	<0.001
TSNIT average (μm)	52.9±4.7	41.7±8.1	<0.001
Superior average (μm)	63.7±5.5	48.0±11.7	<0.001
Inferior average (μm)	59.8±7.3	46.8±10.2	<0.001
TSNIT SD (μm)	21.2±4.0	14.9±5.3	<0.001
Superior ratio	2.9±0.9	2.1±0.8	<0.001
Inferior ratio	3.0±0.9	2.4±0.8	<0.001
Superior/nasal	2.3±0.5	1.8±0.6	<0.001
Max modulation	2.2±0.9	1.6±0.8	<0.001
Superior max (μm)	73.2±8.1	55.2±15.2	<0.001
Inferior max (μm)	76.3±9.4	61.6±13.8	<0.001
Ellipse mod	3.6±1.5	2.8±1.2	<0.001
NSA	0.127±0.016	0.078±0.036	<0.001
NIA	0.132±0.026	0.091±0.031	<0.001

NFI nerve fiber indicator, *TSNIT* ellipse (temporal, superior, nasal, inferior, temporal), *NSA* normalized superior area, *NIA* normalized inferior area

*t test after Bonferroni correction for multiple comparisons; α is approximately 0.0036

Table 3 Values of the GDx variable corneal compensator (VCC) parameters with areas under the receiver operating characteristic (AUROC) curves and sensitivity at a fixed high (≥95%) and moderate (≥80%) specificity

	AUROC (SE)	Specificity ≥95%	Specificity ≥80%
NFI	0.938 (0.022)	79.7	89.8
TSNIT average	0.897 (0.028)	61.0	84.7
NSA	0.879 (0.037)	71.2	86.4
Superior average	0.877 (0.036)	66.1	84.7
Inferior average	0.852 (0.034)	59.3	74.6
NIA	0.850 (0.039)	61.0	74.6
Superior maximum	0.837 (0.039)	61.0	79.7
TSNIT SD	0.830 (0.039)	59.3	79.7
Inferior maximum	0.811 (0.040)	47.5	66.1
Superior ratio	0.755 (0.044)	32.2	61.0
Superior/nasal	0.730 (0.047)	23.7	54.2
Inferior ratio	0.692 (0.047)	22.0	52.5
Maximum modulation	0.683 (0.048)	25.4	44.1
Ellipse modulation	0.662 (0.049)	22.0	45.8

NFI nerve fiber indicator, *TSNIT* ellipse (temporal, superior, nasal, inferior, temporal), *NSA* normalized superior area, *NIA* normalized inferior area

Table 4 Positive and negative likelihood ratios (LR) (with 95% CIs) for nerve fiber indicators (NFI) at four different cutoff values[a]

	NFI cutoff value			
	20	25	30	35
+LR (95% CI)	1.6 (1.29–1.91)	4.8 (2.8–8.0)	17.6 (5.8–53.6)	23.7 (6–93.5)
−LR (95% CI)	0.08 (0.02–0.36)	0.15 (0.07–0.29)	0.19 (0.11–0.33)	0.28 (0.18–0.43)

NFI range	Interval LR (95% CI)	Subjects in each category (%)
0–20	0.08 (0.02–0.36)	27 (22)
21–25	0.20 (0.08–0.48)	33 (27)
26–35	0.99 (0.43–2.28)	19 (15)
36–40	3.31 (0.35–30.91)	4 (3)
>40	45.20 (6.25–310.6)	41 (33)

[a]Interval likelihood ratios (95% confidence intervals) for NFI at different ranges of values

their 95% CI according to the method proposed by Simel et al. [23].

Statistical analysis was performed using SPSS version 12.0 (SPSS Inc., Chicago, IL, USA). Each patient was fully aware about the aim of the study and signed an informed consent to participate. All methods were approved by internal Ethics Committee and adhered to the tenets of the Declaration of Helsinki for research involving human subjects.

Results

One hundred forty-one eyes were considered originally, but 11 (7.8%) presented atypical patterns on the retardation map, four (2.8%) did not pass the four-scan quality check or saw their RNFL readings flagged as "incompatible with normative database," and two (1.4%) had poor fixation and were excluded. The remaining 124 eyes (87.9%) fulfilled inclusion and exclusion criteria and were enrolled. Among them, 65 were classified as healthy and 59 as glaucomatous on the basis of AAP results. The mean values for age, MD, and PSD were significantly different between the two groups ($p<0.001$). These values are collected in Table 1. According to the Hodapp–Parrish–Anderson classification of perimetric defect [9], 21 eyes (36%) had early, 15 (25%) moderate, and 23 (39%) severe defects. In Table 2, mean values (± SD) for each parameter are shown separately for healthy and glaucomatous eyes. All parameters were significantly different between the two groups ($p<0.001$). In Table 3, AUROCs (SE) for all parameters are presented, as well as sensitivity values at fixed specificity value ≥80% and ≥95%. In Table 4, positive and negative LRs for the NFI at cutoff values of 20, 25, 30, and 35 are shown, as well as interval LRs for different range values of the same parameter.

Discussion

Other than on clinical examination of optic disc and on AAP, modern diagnosis of glaucoma can benefit from instrumentations that evaluate optic disc topography and peripapillary RNFL thickness. Since its introduction, SLP has gone through a constant technical improvement. Earlier GDx versions were coupled with FCC, but evaluation of their diagnostic ability produced conflicting results [2, 8, 26, 31]. Incomplete compensation of anterior segment birefringence in some eyes [7, 30] produced spurious measurements of RNFL thickness so that some parameters were overestimated up to 20 μm [5] and overlapping between healthy and glaucomatous eyes occurred [3, 5, 14, 25]. Customized compensation of anterior segment birefringence improved diagnostic ability and structure–function relationship significantly [3, 5, 14, 15, 18–21, 25].

In the present study, we evaluated the performance of a commercially available version of GDx-VCC in separating healthy from glaucomatous eyes. Other authors recently did the same using a modified version of the nerve fiber analyzer (NFA) on which FCC was substituted by a prototype of VCC [5, 8, 14, 21, 25, 29]. To the best of our knowledge, only one paper has assessed the performance of a commercially available instrument previously [15].

In our population comprised of age-matched healthy and glaucomatous eyes, all parameters provided by SLP-VCC resulted in a significant difference between the two groups ($p<0.001$, t test) (Table 2), even after Bonferroni correction. New parameters provided by SLP-VCC software as NFI, NSA, NIA, and TSNIT SD offered a good perspective in improving the machine's ability to separate healthy from glaucomatous eyes. Moreover, in our study population, parameters presented in the first page of the printout appear reliable since four of them (NFI, TSNIT average, SA, and IA) stand at the top positions in the AUROC values list (Table 3).

Previous papers conducted with a modified NFA coupled with a VCC had AUROC for their best parameter ranging from 0.83 to 0.87 [8, 14, 25, 29], but they could not evaluate new parameters as NFI, NSA, NIA, and TSNIT average. Values of AUC (Table 3) indicate NFI as the best performing parameter (0.938, Fig. 1) followed by TSNIT average (0.897) and NSA (0.879). Medeiros et al. [15] obtained the best AUC for NFI (0.91), NIA (0.86), and TSNIT average (0.85). More recently, Reus and Lemij [19] obtained an AUC of 0.98 for NFI. Such differences may

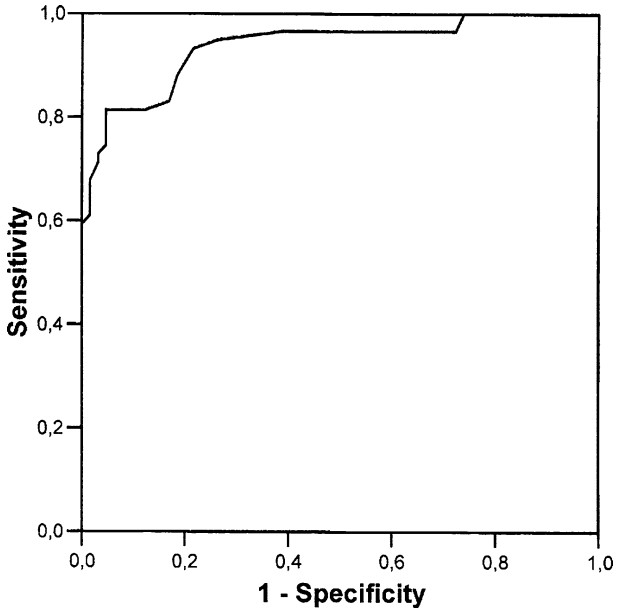

Fig. 1 Receiver operating characteristic (ROC) curve for nerve fiber indicator (NFI) constructed plotting sensitivity versus 1-specificity. Area under the ROC curve is 0.938 (SE 0.022).

be attributed to the fact that this latter study dealt with younger patients with visual field loss of greater average severity (55.5% of eyes had severe defects) with respect to both our study and the one by Medeiros et al. [15] (39% and 15%, respectively). Moreover, at a specificity ≥95%, NFI sensitivity in our study was nearly 80% (Table 3).

Papers dealing with accuracy of diagnostic tests tend to provide LR values with increasing frequency at the expense of sensitivity and specificity. When continuous variables are forced into dichotomous classification, as it is when sensitivity and specificity are employed, there may be some loss of valuable information, and a distorted interpretation of data may occur. When LRs are used, especially interval LR, the advantage is that they are not influenced by the format used to express test results (dichotomous, ordinal, continuous data) [6]. The analysis of LRs for the best parameter, i.e., NFI (Table 4) highlighted that at manufacturer-suggested cutoff value of 30, positive LR is 17.6 (95% CI 5.8–53.6), indicating large effect on posttest probability. On the contrary, negative LR testified a similar effect (0.08, 95% CI 0.02–0.36) at a cutoff value of 20.

In the eyes in our study, assessment of interval LRs (Table 4) indicated a value of 0.99 for a range of NFI values comprised between 26 and 35, indicating that these values may occur with similar probability both in healthy and affected eyes. A large effect on posttest probability was noted for NFI values ≤20 or >40. This range of values is located halfway between corresponding values <35 or ≥44 described by Reus and Lemji and <15 or >50 reported by Medeiros et al. [15]. Differences between studies probably reflect again the effect of different average severity of the disease. As the percentage of eyes with early glaucomatous visual field loss increases, there is a higher probability to find eyes with NFI values <30 (that is supposed to separate "within normal limits" from "borderline" eyes). In our glaucomatous population, 11 eyes (18.6%) had NFI <30 and nine had an early field defect. Leaving out from statistical evaluation all 21 eyes with early glaucoma and considering only those with moderate and severe visual field loss, AUC for NFI increased up to 0.963 (SE 0.021), and at a cutoff value of 30, positive LR became 19.9 (95% CI 6.6–60.5) and negative LR 0.08 (95% CI 0.03–0.25).

Data from previous papers [3, 5, 14, 15, 25] and from our study reassign a role of prominence to parameters that quantify RNFL thickness. Ratios and modulation parameters showed a better diagnostic accuracy than thickness ones on SLP-FCC [7, 29], but in our study, their ROC curves lie the bottom half of the list, and values are no better than 0.755 on GDx-VCC (Table 3).

In conclusion, the availability of SLP-VCC represents a significant improvement in the diagnosis of glaucoma with respect to SLP-FCC. A commercially available version of GDx-VCC allowed us to scan and measure successfully the peripapillary RNFL in 88% of studied eyes. In our opinion, however, the role of this device may be further enhanced by improving its sensitivity in correctly identifying eyes with early RNFL defects. This could be achieved not only by analyzing single parameters but most probably through a standardized, thorough evaluation of the whole GDx-VCC printout.

Another issue has never been faced is the SLP-VCC role in preperimetric glaucoma assessment: All available studies have compared healthy eyes with eyes with reproducible glaucomatous visual field defects. If a large multicenter study on glaucoma suspects is performed, it will be possible to determine if SLP-VCC may play a key role in the diagnosis of very early glaucoma.

References

1. Bagga H, Greenfield DS, Feuer WJ, Knighton RW (2003) Scanning laser polarimetry with variable corneal compensation and optical coherence tomography in normal and glaucomatous eyes. Am J Ophthalmol 135:521–529

2. Bowd C, Zangwill LM, Berry CC, Blumenthal EZ, Vasile C, Sanchez-Galeana C et al (2001) Detecting early glaucoma by assessment of retinal nerve fiber layer thickness and visual function. Invest Ophthalmol Vis Sci 42:1993–2003

3. Bowd C, Zangwill LM, Weinreb RN (2003) Association between scanning laser polarimetry measurements using variable corneal polarization compensation and visual field sensitivity in glaucomatous eyes. Arch Ophthalmol 121:961–966

4. Chen YY, Chen PP, Xu L, Ernst PK, Wang L, Mills RP (1998) Correlation of peripapillary nerve fiber layer thickness by scanning laser polarimetry with visual field defects in patients with glaucoma. J Glaucoma 7:312–316
5. Choplin NT, Zhou Q, Knighton RW (2003) Effect of individualized compensation for anterior segment birefringence on retinal nerve fiber layer assessment as determined by scanning laser polarimetry. Ophthalmology 110:719–725
6. Gallagher EJ (2003) Evidence-based emergency medicine/editorial: the problem with sensitivity and specificity. Ann Emerg Med 42:298–303
7. Greenfield DS, Knighton RW, Huang XR (2000) Effect of corneal polarization axis on assessment of retinal nerve fiber layer thickness by scanning laser polarimetry. Am J Ophthalmol 129:715–722
8. Greenfield DS, Knighton RW, Feuer WJ, Schiffmann JC, Zangwill LM, Weinreb RN (2002) Correction for corneal polarization axis improves the discriminating power of scanning laser polarimetry. Am J Ophthalmol 134:27–33
9. Hodapp E, Parrish RK II, Anderson DR (1993) Clinical decisions in glaucoma. Mosby Year Book, St. Louis, pp 52–61
10. Jaeschke R, Guyatt GH, Sackett DL, Evidence-Based Medicine Working Group (1994) User's guides to the medical literature, III: how to use an article about a diagnostic test, B: what are the results and will they help me in caring for my patients? JAMA 271:703–707
11. Kass MA, Heuer DK, Higginbotham EJ, Johnson CA, Keltner JL, Miller JP et al (2002) The ocular hypertension treatment study: a randomized trial determines that topical ocular hypotensive medication delays or prevents the onset of primary open-angle glaucoma. Arch Ophthalmol 120:701–713
12. Knighton RW, Huang XR (2002) Linear birefringence of the central human cornea. Invest Ophthalmol Vis Sci 43:82–86
13. Kwon YH, Hong S, Honkanen RA, Alward WL (2000) Correlation of automated visual field parameters and peripapillary nerve fiber layer thickness as measured by scanning laser polarimetry. J Glaucoma 9:281–288
14. Medeiros FA, Zangwill LM, Bowd C, Bernd AS, Weinreb RN (2003) Fourier analysis of scanning laser polarimetry measurements with variable corneal compensation in glaucoma. Invest Ophthalmol Vis Sci 44:2606–2612
15. Medeiros FA, Zangwill LM, Bowd C, Weinreb RN (2004) Comparison of the GDx VCC scanning laser polarimeter, HRT II confocal scanning laser ophthalmoscope, and stratus OCT optical coherence tomography for the detection of glaucoma. Arch Ophthalmol 122:827–837
16. Pederson JE, Anderson DR (1980) The mode of progressive optic disc cupping in ocular hypertension and glaucoma. Arch Ophthalmol 98:490–495
17. Quigley HA, Addicks EM, Green RW (1982) Optic nerve damage in human glaucoma. III. Quantitative correlation of nerve fiber loss and visual defect in glaucoma, ischemic neuropathy, papilledema, and toxic neuropathy. Arch Ophthalmol 100:135–146
18. Reus NJ, Colen TP, Lemij HG (2003) Visualization of localized retinal nerve fiber layer defects with the GDx with individualized and with fixed compensation of anterior segment birefringence. Ophthalmology 110:1512–1516
19. Reus NJ, Lemij HG (2004) Diagnostic accuracy of the GDx VCC for glaucoma. Ophthalmology 111:1860–1865
20. Reus NJ, Lemij HG (2004) The relationship between standard automated perimetry and GDx VCC measurements. Invest Ophthalmol Vis Sci 45:840–845
21. Schlottmann PG, De Cilla S, Greenfield DS, Caprioli J, Garway-Heath DF (2004) Relationship between visual field sensitivity and retinal nerve fiber layer thickness as measured by scanning laser polarimetry. Invest Ophthalmol Vis Sci 45:1823–1829
22. Shields JR, Chen PP, Mills RP (2002) Topographic mapping of glaucomatous visual field defects to scanning laser polarimetry of the peripapillary nerve fiber layer. Ophthalmic Surg Lasers 33:123–126
23. Simel DL, Samsa GP, Matchar DB (1991) Likelihood ratios with confidence: sample size estimation for diagnostic test studies. J Clin Epidemiol 44:763–770
24. Sommer A, Katz J, Quigley HA, Miller NR, Robin AL, Richter RC et al (1991) Clinically detectable nerve fiber layer atrophy precedes the onset of glaucomatous field loss. Arch Ophthalmol 109:77–83
25. Tannenbaum D, Hoffmann D, Lemij HG, Garway-Heath DF, Greenfield DS, Caprioli J (2004) Variable corneal compensation improves the discrimination between normal and glaucomatous eyes with the scanning laser polarimeter. Ophthalmology 111:259–264
26. Tjon-Fo-Sang MJ, Lemij HG (1997) The sensitivity and specificity of nerve fiber layer measurements in glaucoma as determined with scanning laser polarimetry. Am J Ophthalmol 123:62–69
27. Weinreb RN, Dreher AW, Coleman A, Quigley H, Shaw B, Reiter K (1990) Histopathologic validation of Fourier-ellipsometry measurements of retinal nerve fiber layer thickness. Arch Ophthalmol 108:557–560
28. Weinreb RN, Shakiba S, Sample PA, Shahroknis S, van Horn S, Garden VS et al (1995) Association between quantitative nerve fiber layer measurement and visual field loss in glaucoma. Am J Ophthalmol 120:732–738
29. Weinreb RN, Bowd C, Zangwill LM (2002) Glaucoma detection using scanning laser polarimetry with variable corneal polarization compensation. Arch Ophthalmol 120:218–224
30. Weinreb RN, Bowd C, Greenfield DS, Zangwill LM (2002) Measurement of the magnitude and axis of corneal polarization with scanning laser po larimetry. Arch Ophthalmol 120:901–906
31. Zangwill LM, Bowd C, Berry CC, Williams J, Blumenthal EZ, Sanchez-Galeana C et al (2001) Discriminating between normal and glaucomatous eyes using the Heidelberg retina tomograph, GDx nerve fiber analyzer, and optical coherence tomograph. Arch Ophthalmol 119:985–993
32. Zhou Q, Weinreb RN (2002) Individualized compensation of anterior segment birefringence during scanning laser polarimetry. Invest Ophthalmol Vis Sci 43:2221–2228